Hindawi
International Journal of Photoenergy
Volume 2019, Article ID 1069308, 7 pages
https://doi.org/10.1155/2019/1069308

Research Article

The Optimized Thickness of Silver Doping on CdS/CdSe for Quantum Dot-Sensitized Solar Cell

Ha Thanh Tung[1] **and Dang Huu Phuc**[2,3]

[1]*Institute of Research and Development, Duy Tan University, Da Nang, Vietnam*
[2]*Laboratory of Applied Physics, Advanced Institute of Materials Science, Ton Duc Thang University, Ho Chi Minh City, Vietnam*
[3]*Faculty of Applied Sciences, Ton Duc Thang University, Ho Chi Minh City, Vietnam*

Correspondence should be addressed to Dang Huu Phuc; danghuuphuc@tdtu.edu.vn

Received 14 June 2019; Revised 14 October 2019; Accepted 27 November 2019; Published 29 December 2019

Guest Editor: Jingkun Fang

Overall, CdSe:Ag^+ quantum dots were prepared by the successive ionic layer absorption and reaction method using two solutions: mixing molar concentrations of 0.003 mM $AgNO_3$ and a $Cd(CH_3COO)_2{\cdot}2H_2O$ anion to make solution 1 and 2.27 g Se powder and 0.6 M Na_2SO_3 were dissolved in 100 ml deionized water, solution 2. The FTO was coated with TiO_2 nanoparticles and then was dipped in both solutions, which created a FTO/TiO_2/CdSe:Ag^+ photoanode with a thickness of 1 layer to 4 layers. The layers of the CdSe:Ag^+ film show an effect on the morphology, crystalline structure, optical properties, and photovoltaic through optical and photovoltaic measurements. Finally, the performance of the device based on a FTO/TiO_2/CdSe:Ag^+ photoanode with the different thickness increased significantly to exactly 3.96%. Moreover, in the pattern of an explanation of the optical and photovoltaic properties of materials, we use Tauc's theory to determine the band gap, the conduction band, and the valence band.

1. Introduction

Quantum dot-sensitized solar cells (QDSSCs) are prominently becoming as a dye sensitized for the 3rd generation solar cells due to low cost fabrication technology, high photostability, the controlled sizes [1], higher absorption coefficient [2], and the multiple exciton generation [3]. However, the QDSSCs have reached approximately 13% performance, which is lower than the theory limits [4]. Recently, plenty of quantum dots (QDs) like CdS, CdSe, CdTe [5], and PbS [6] have been widely applied in the QDSSCs because of their unique properties [7]. It is noticeable that the CdS and CdSe QDs have attracted considerable interest due to their optical property stability [8], a higher conduction band (CB) than that of TiO_2 [9], low resistivity [10], and wide absorbed spectrum [11]. However, this result was still low compared with that of the dye-sensitized solar cells (DSSCs). The structure tandem as CdS/CdSe cosensitized was widely investigated due to their wide absorption spectrum, the shift of the absorption peak toward the visible region, and improvement of the CB of a cosensitized system compared to that of TiO_2 nanoparticles. The performance of this device based on a cosensitized system was approximately 4% [9], but it was still low compared to that of DSSCs, mostly due to the trapped and recombined TiO_2/QDs/electrolyte tripple interfaces [12].

In recent times, metal ions doped into the QDs can be replaced by single QDs and a cosensitized system to reduce achievable recombination [13–23] because it can be improved by charge collection and transfer process. In addition, metal ions are famous for its lowest resistance and large mobility. For example, Nguyen and colleagues achieved a performance of 4.22% as Cu^{2+} ion doped into CdSe QDs due to its good optical and magnetic properties as compared with each other [13]. The improved properties can be archived by doping metal in QDs like Ref [14, 15], [19–23] that can boost absorption of photons and the current density of devices.

In this work, Ag^+ ions were doped on CdSe QDs to study the properties of devices when the thickness of the CdSe:Ag^+ layers change while the molar concentration of Ag^+ ions doped on CdSe nanoparticles was optimized at 3% for the champion device. Moreover, resistance dynamic

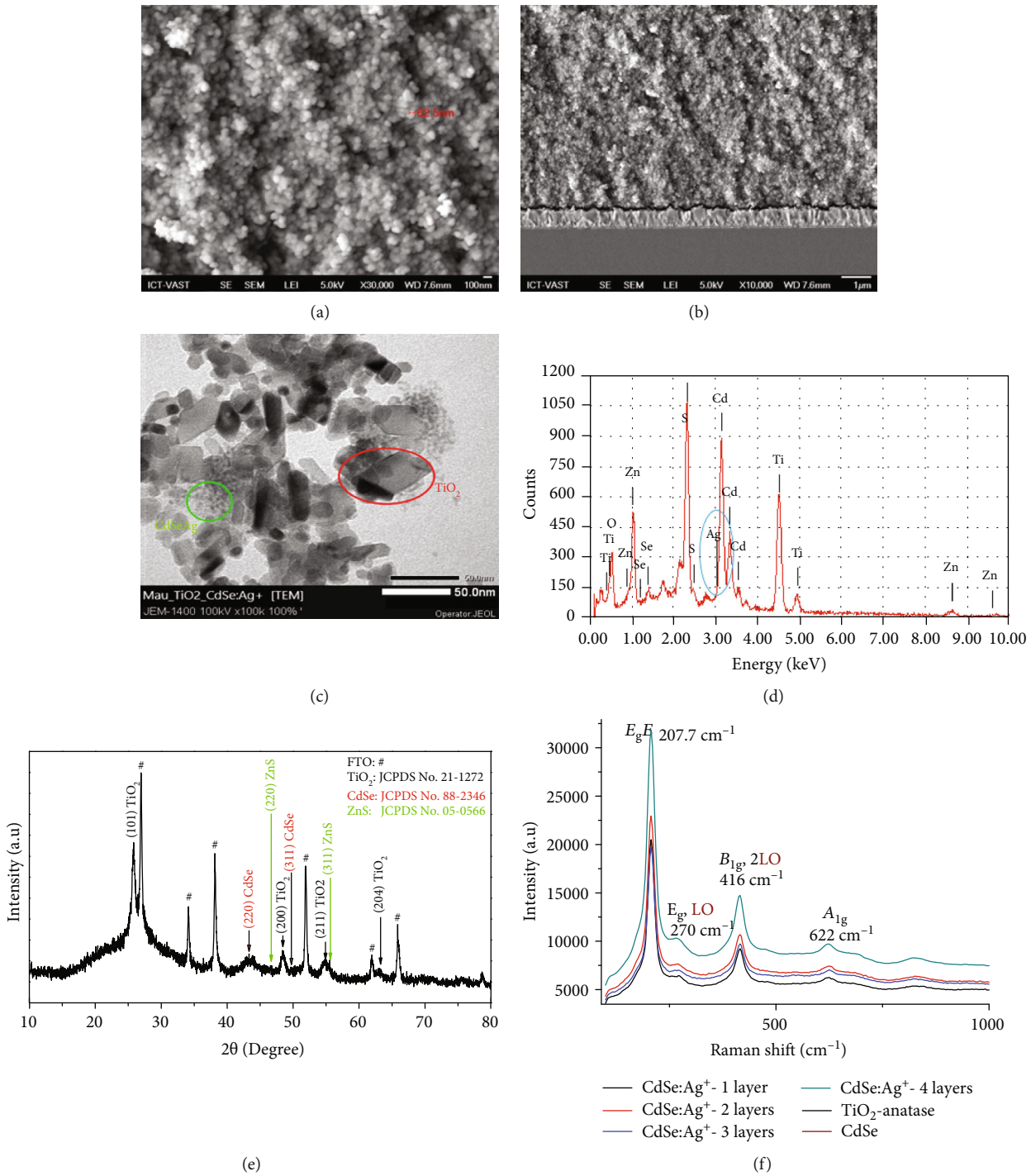

Figure 1: (a) FESEM image, (b) Cross-section, (c) TEM, (d) EDX spectrum, and (e) XRD pattern of TiO_2/CdSe:Ag^+(3%)/ZnS and (f) the Raman spectrum of photoanode with the different thickness.

was determined from an experiment J-V curve compared with that of electrochemical impedance spectra.

2. Experiment

2.1. Materials. Na_2SO_3, NaOH, $Cd(CH_3COO)_2{\cdot}2H_2O$, $Zn(NO_3)_2$, $Na_2S{\cdot}9H_2O$, methanol, Se powder, $TiCl_4$, and $AgNO_3$ were bought from Merck, and the fluorine-doped tin oxide was bought from Dyesol.

2.2. Preparation. TiO_2 paste was purchased from Dyesol in Australia with 20 nm sized average. The fluorine-doped tin oxide (FTO) was coated with TiO_2 layers by doctor blade and then heated to 400°C for 5 minutes, 450°C for 5 minutes, 490°C for 5 minutes, and 500°C for 30 minutes [24]. It was

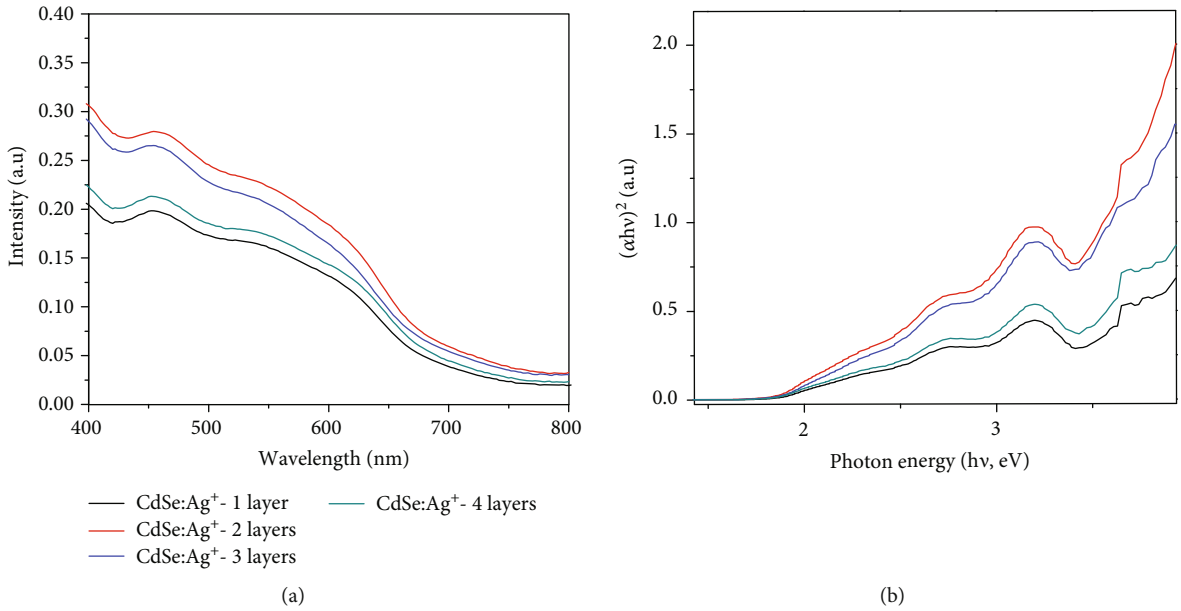

Figure 2: (a) UV-Vis spectra and (b) $(\alpha h\nu)^2$ vs. $(h\nu)$ curves of TiO_2/CdSe:Ag^+ with thickness from 1 layer to 4 layers.

then immersed in 40 mM $TiCl_4$ for 30 minutes at 70°C. Finally, the postheating treatment of TiO_2 film was carried out at 500°C for 30 minutes.

The TiO_2/CdSe:Ag^+ film: the TiO_2 film was dipped into a Cd^{2+} solution (molar concentrations of 0.001 mM, 0.002 mM, 0.003 mM, 0.004 mM, and 0.005 mM of $AgNO_3$ were mixed) and 0.5 M Cd^{2+} solution (13.3 g $Cd(CH_3COO)2{\cdot}2H_2O$ was dissolved in 100 ml ethanol) for 5 minutes, rinsed 3 times with ethanol, and dried in the air. It was then dipped into Se^{2+} ions (2.27 g Se powder, 0.6 M Na_2SO_3 were dissolved in 100 ml deionized water and added 5 ml NaOH 1 M). Finally, we got 0.3 M Se^{2+} solution at 50°C for 5 minutes, rinsed 3 times with deionized water for 1 minute, which was noticed one cycle. This process was repeated a total of 3 times SILAR.

The coated ZnS passivation: the TiO_2/CdSe:Ag^+ film was dipped in a mix of 0.2 M $Zn(NO_3)_2$ with deionized water for 1 min and rinsed with deionized water to remove ligands. Nextly, it was dipped in a solution of 0.2 $Na_2S{\cdot}9H_2O$ and methanol for 1 minute and rinsed with methanol to get a 1 cycle of SILAR. This process was repeated a total of 3 times SILAR. The detailed preparation process of electrolyte and counter electrode is listed in Ref [13].

2.3. Characterization. The scanning electron microscopy (SEM) with a JEOL 7500F high-resolution scanning electron microscope was used to determine the morphology of the films. Their characteristic and structure were confirmed using an X-ray diffractometer (Philips, PANalytical X'Pert, CuKα radiation), and optical properties are recorded by using a JASCO V-670. The J-V curves were measured (2400 Series SourceMeter, Keithley Instruments) under simulated AM 1.5 G sunlight at 100 mW·cm^{-2}. The active area of the solar cell measured under AM 1.5 G is 0.192 cm^2. The J-V scans were measured forward bias at a scan rate of 5 mV·s^{-1}. The electrochemical impedance spectroscopy (EIS) Series G 750 was measured under dark conditions at a forward bias of 0.75 V within the frequency range of 100 kHz to 0.1 Hz.

Table 1: The parameters of CdSe:Ag^+ films are determined using Tauc plots and UV-Vis spectra.

Samples	E_g (eV)	X (eV)	CB (eV)	VB (eV)
CdSe	2.16	5.102	-4.065	-6.225
CdSe:Ag^+ (1 layer)	2.0	5.102	-3.766	-5.766
CdSe:Ag^+ (2 layers)	1.96	5.102	-3.786	-5.746
CdSe:Ag^+ (3 layers)	1.96	5.102	-3.786	-5.746
CdSe:Ag^+ (4 layers)	1.95	5.102	-3.791	-5.741

3. Results and Discussion

In order to determine the morphology of the films, we used the FE-SEM images and cross-sectional of the previous paper. The result shows that the porous TiO_2 nanoparticles look like a sphere and the size average of 62.5 nm and thickness of the TiO_2/CdSe:Ag^+ were about 13 μm (Figure 1(b)) [24]. This result is also confirmed by TEM (shown in Figure 1(c)). The CdSe:Ag^+ nanoparticles in the film were not observed in the FE-SEM, but they can be clearly seen from TEM image. The average size of CdSe:Ag^+ nanoparticles was determined from Figure 1(c) approximately several nanomet. Moreover, the EDX spectrum of the photoelectrode was recorded in Figure 1(d). It is immediately obvious that the peak at 3 keV can be assigned to the characteristic of Ag^+ ions. The result shows that Ag^+ ions would be doped in CdSe QDs and effected on the photovoltaic. The typical XRD pattern of the photoelectrode was obtained in a vacuum environment at 200°C with the molar atomic of Ag^+ ion and CdSe QDs (3%) (shown in Figure 1(e)). The XRD pattern was recorded many diffraction peaks in a 2θ range

Table 2: The values of J-V curves and EIS with thickness from 1 layer to 4 layers.

QDSSCs	J_{SC} (mA/cm^2)	FF	V_{OC} (V)	η (%)	R_S (Ω)	R_{ct1} (Ω)	R_{ct2} (Ω)	τ_n (ms)	C_μ (μF)
CdSe:Ag$^+$ (1 layer)	7.46	0.44	0.38	1.22	21.29	30.77	18.92	2.38	12.25
CdSe:Ag$^+$ (2 layers)	15.36	0.41	0.50	3.96	21.3	46.54	26.94	6.86	72.66
CdSe:Ag$^+$ (3 layers)	12.22	0.42	0.44	2.83	24.34	193.1	81.46	5.19	86.72
CdSe:Ag$^+$ (4 layers)	9.89	0.46	0.47	2.11	19.44	293.5	82.6	5.51	39.70

from the 20° to 70°, which exhibits the structure of materials. By comparing the observed XRD patterns for the prepared film, Figure 1(e) shows the characteristic peaks of CdSe QDs, which correspond to the standard JCPDS card No. 88-2346 for the zinc blende structure and standard JCPDS card No. 05-0566 for the cubic phase of ZnS passivation. This result is consistent with that observed in the zinc blende phase [25, 26]. Figure 1(f) for the Raman spectrum of the completed QDSSCs with thickness between 1 layer and 4 layers always gives information about the TiO_2 anatase modes at 207.7 cm^{-1}, 416 cm^{-1}, and 622 cm^{-1} positions [27] and the TiO_2/CdSe:Ag$^+$ cubic at 207.7 cm^{-1}, 270 cm^{-1}, 416 cm^{-1}, and 622 cm^{-1} positions. All peaks shifted toward the high frequency because of the strengthening CdSe:Ag$^+$-TiO_2 associate as in those of CdSe-TiO_2 associate.

To research the effect of thickness on optical properties of TiO_2/CdSe:Ag$^+$ films, we use the UV-Vis spectra. We can see the differences from Figure 2(a) such as: while the thickness varied from 1 layer to 4 layers, the diagram describes an increase absorption intensity and shift of the absorption peak toward long wave because of Ag$^+$ trapping dopant inside the band gap of CdSe QDs [28–31]. Figure 2(b) shows the Tauc plots of CdSe:Ag$^+$ layers, and its parameters are shown in Table 1. The E_g of CdSe:Ag$^+$ nanoparticles decreased from 2.0 eV for 1-layer photoelectrode to 1.95 eV for 4-layer photoelectrode. This result shows that there was a strong influence of the thickness on the E_g of CdSe:Ag$^+$ film [32].

In order to study the photovoltaic characteristic, we conducted a set of the QDSSCs with different thickness (an active area of 0.38 cm^2) from 1 layer to 4 layers, and their parameters are listed in Table 2. When doping, open circuit parameters, short circuit currents, and efficiency are increased because the CB level of CdSe:Ag$^+$ layers raised higher than that of TiO_2 nanoparticles (listed in Table 1 and see in Figure 3) [24]. In the same optical properties, while 1.22% of performance for CdSe:Ag$^+$ 1 layer was recorded, the performance of devices for CdSe:Ag$^+$ 2 layers was sharply raised, at 3.96%. On the other hand, the performance of QDSSCs for CdSe:Ag$^+$ 2 layers and CdSe:Ag$^+$ 4 layers, which was recorded at 3.96% and 2.11%, respectively. It is obvious that the concentration impurities affect the properties of CdSe nanoparticles. Briefly, the highest performance was approximately 3.96%, corresponding to 3% of Ag$^+$ concentrations and 2 layers of CdSe:Ag$^+$ film. Figure 4 shows data on the CB and the VB of TiO_2 semiconductor and CdSe:Ag$^+$ nanoparticles; some parameters are referenced from Ref [33, 34]. Generally, the charges are not easy to transfer from the CB of QDs to TiO_2 oxide because -4.5 eV of the CB level for CdSe bulk was slightly lower than -4.3 eV of the CB level for TiO_2

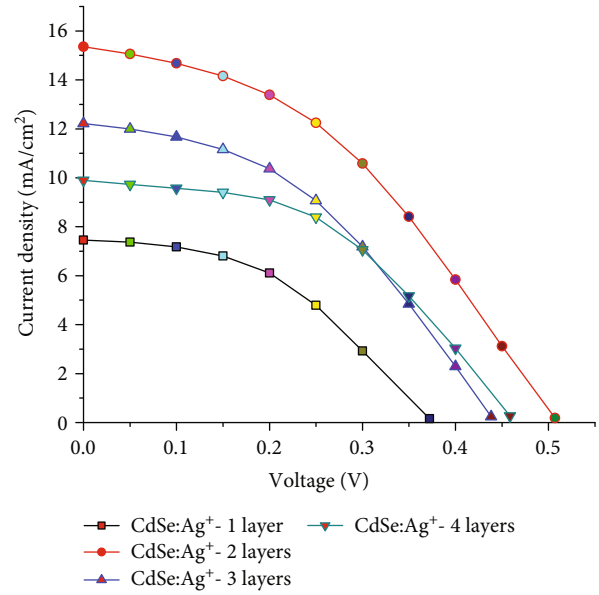

Figure 3: Photocurrent density-voltage (J-V) curves of QDSSCs with different thickness from 1 layer to 4 layers.

semiconductor bulk [22]. Therefore, in this work, Ag$^+$ ion was doped on CdSe nanoparticles to improve the conduction band and the absorption spectra. The graph gives information about the conduction band, bandgap, and valence band of CdSe:Ag$^+$ nanoparticles, which was calculated from Tauc's theory. -4.102 eV of the CB level for CdSe nanoparticles 1 layer and -3.786 eV of the CB level for CdSe nanoparticles 4 layers raised higher than those of the CB of TiO_2 nanoparticles (Figure 3). Finally, the charges can be easily removed from QDs to TiO_2. That is why the conversion efficiency and current density for device champion is high, at 3.96% and at 15.36 mA, respectively.

The EIS curves were used to determine the resistance dynamic in the QDSSCs (shown in Figure 5(b)) with different layers; the parameter values are shown in Table 2. Generally, there are two semicircles in the EIS curve, one small semicircle at high frequency of the resistance through polyelectrolyte/Cu_2S surface (R_{ct1}) and one large semicircle at low frequency of the diffuse resistance through TiO_2 film and TiO_2/CdSe:Ag$^+$ surface (R_{ct2}) [35]. In the recorded EIS curve, the fit process used Nova software to determine the parameters as the resistances (R_{ct1} and R_{ct2}), the capacitance (C_μ), and the lifetime (τ_n). The formulas of the lifetime and the capacitance are determined by $\tau_n = 1/(2\pi f_{min})$, and $C_\mu = \tau_n/R_{ct2}$ (shown in Table 2). Overall, Table 2 shows data

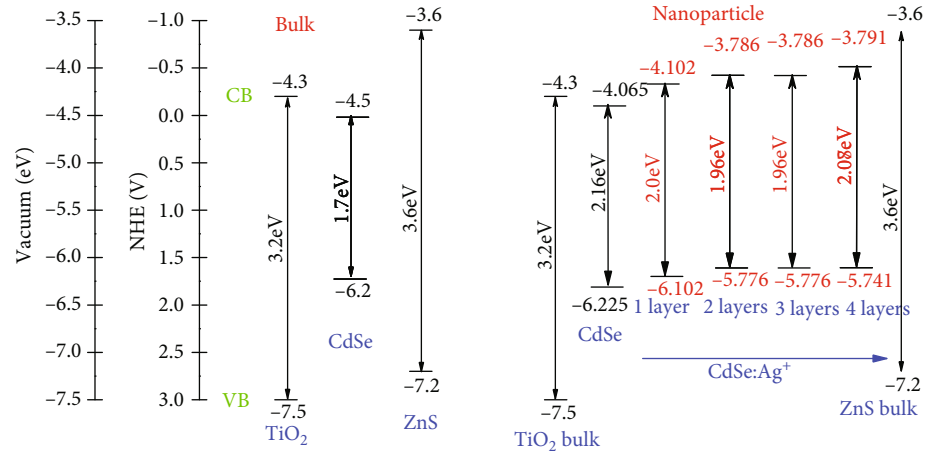

FIGURE 4: A schematic diagram for the band alignment in bulk materials and TiO_2/CdSe:Ag^+ photoanode.

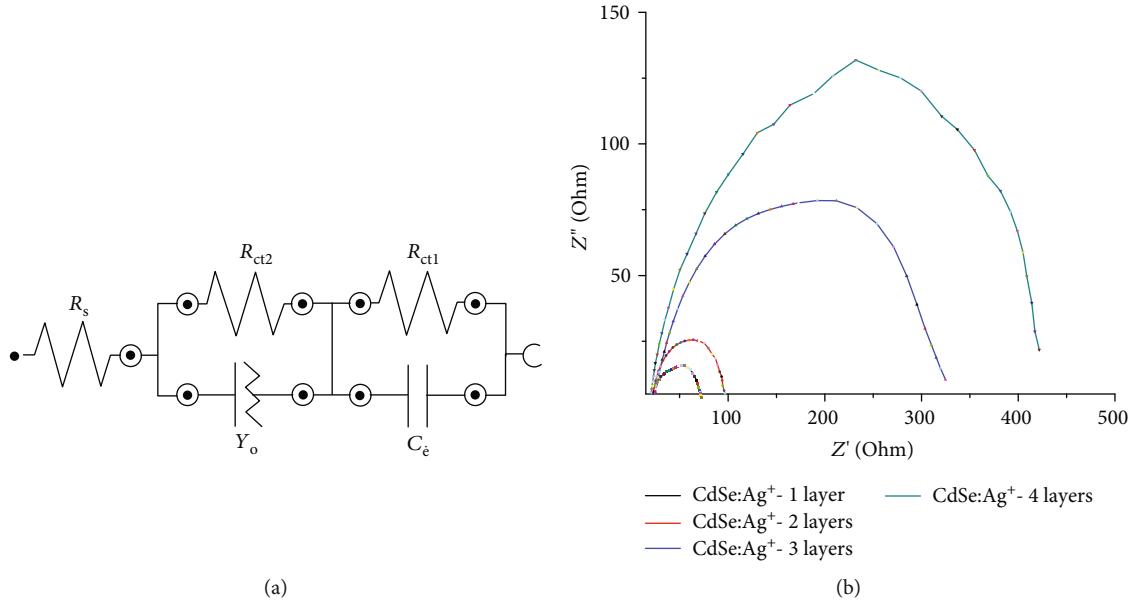

FIGURE 5: (a) The circuit diagram of devices and (b) Nyquist plots of QDSSCs with the different layers.

on the proportion of the device based on TiO_2/CdSe:Ag^+ photoelectrodes with the thickness of 1 layer to 4 layers, which affects the dynamic parameters of the photovoltaic properties. While the capacitance and lifetime of the excited charge was higher, the 293.5 Ω of R_{ct1} for CdSe:Ag^+ 4-layer photoelectrode and 82.6 Ω of R_{ct2} for CdSe:Ag^+ 4-layer photoelectrode were always higher than those of R_{ct1} and R_{ct2} for CdSe:Ag^+ 1-layer photoelectrode, at 30.77 Ω and 18.92 Ω, respectively [34]. Briefly, the improvement of energy band structure of CdSe nanoparticles as raising the conduction band reduces recombination and trapping surfaces, shifting the absorption spectra toward longwave due to the Ag^+ dopant, which appeared inside the band gap of CdSe nanoparticles. This result is also consistent with the results of Ref [33, 34, 36–38].

4. Conclusions

In conclusion, the device based on TiO_2/CdSe:Ag^+ photoanode with cycles changing from 1 to 4 was successfully prepared using the SILAR method with the obtaining highest efficiency of 3.96%. This result was also confirmed by the corporation of Ag^+ ion in photoelectrode, the changed sizes of QDs. The increase of the CB of the CdSe:Ag^+ QDs was caused by improvement of the performance. We also optimized the optical (E_g and lifetime τ), photovoltaic, and electrochemical properties through the optimized thickness of CdSe:Ag^+ films, thereby raising the efficiency of 3.96%. In order to compare with each other, we determined the values of dynamic resistances by EIS (R_s, R_{ct1}, R_{ct2}, and C_μ).

Data Availability

The analysis data used to support the findings of this study are included within the article. The supplementary material data used to support the findings of this study are included within the supplementary information files.

Conflicts of Interest

The authors declare no competing interests.

Acknowledgments

The authors would like to thank University of Science, VNU-HCM, Vietnam.

Supplementary Materials

Supplemental Figure 1: (a) FESEM image, (b) Cross-section, and (c) XRD pattern of TiO_2/CdSe:Ag+(3%)/ZnS and (d) the Raman spectrum of QDSSCs with the different thickness. The morphology of preparing as-photoelectrodes with 3% doping concentration could be obtained from FE-SEM. In addition, the compositions and structure of films could be investigated from EDX and Raman spectra. In general, this is the main data sets, which provided all information about the morphology, sizes, thickness of a sandwich layer, and structure of preparing as-photoelectrodes. Supplemental Figure 2: (a) UV-Vis spectra and (b) $(\alpha h\nu)2$ vs. $(h\nu)$ curves of TiO_2/CdSe:Ag+ with thickness from 1 layer to 4 layers. This is the supplementary material, which supports for us to determine the band gap of sample as getting the peak of UV-Vis spectra, in particular, calculate the conduction band and valence band of material. Supplemental Figure 3: photocurrent density-voltage (J-V) curves of QDSSCs with different thickness from 1 layer to 4 layers. The performance of the quantum dot-sensitized solar cells could be obtained from the photocurrent density-voltage curves. This results support for the discussion from the electrochemical impedance spectra. Supplemental Figure 5: Nyquist plots of QDSSCs with the different layers. The data set obtained from the electrochemical impedance spectra such as Nyquist curves and Bode phase. They used to determine resistance dynamic, lifetime, and capacitances of the photoelectrodes to correlate with the shift of excited electrons from quantum dots to TiO_2 nanoparticles, the diffusion of electrons. *(Supplementary Materials)*

References

[1] Z. A. Peng and X. Peng, "Formation of high-quality CdTe, CdSe, and CdS nanocrystals using CdO as precursor," *Journal of the American Chemical Society*, vol. 123, no. 1, pp. 183-184, 2001.

[2] M. C. Beard, "Multiple exciton generation in semiconductor quantum dots," *Journal of Physical Chemistry Letters*, vol. 2, no. 11, pp. 1282–1288, 2011.

[3] E. H. Sargent, "Infrared quantum dots," *Advanced Materials*, vol. 17, no. 5, pp. 515–522, 2005.

[4] S. Jiao, J. Du, Z. Du et al., "Nitrogen-doped mesoporous carbons as counter electrodes in quantum dot sensitized solar cells with a conversion efficiency exceeding 12%," *Journal of Physical Chemistry Letters*, vol. 8, no. 3, pp. 559–564, 2017.

[5] X. Shen, J. Jia, Y. Lin, and X. Zhou, "Enhanced performance of CdTe quantum dot sensitized solar cell *via* anion exchanges," *Journal of Power Sources*, vol. 277, pp. 215–221, 2015.

[6] A. N. Jumabekov, T. D. Siegler, N. Cordes et al., "Comparison of solid-state quantum-dot-sensitized solar cells withex Situandin SituGrown PbS quantum dots," *The Journal of Physical Chemistry C*, vol. 118, no. 45, pp. 25853–25862, 2014.

[7] J. Duan, Q. Tang, B. He, and L. Yu, "Efficient In_2S_3 Quantum dot–sensitized Solar Cells: A Promising Power Conversion Efficiency of 1.30%," *Electrochimica Acta*, vol. 139, pp. 381–385, 2014.

[8] L. Li, X. Zou, H. Zhou, and G. Teng, "Cu-Doped-CdS/In-Doped-CdS Cosensitized Quantum Dot Solar Cells," *Journal of Nanomaterials*, vol. 2014, Article ID 314386, 8 pages, 2014.

[9] Y. L. Lee and Y. S. Lo, "Highly Efficient Quantum-Dot-Sensitized Solar Cell Based on Co-Sensitization of CdS/CdSe," *Advanced Functional Materials*, vol. 19, no. 4, pp. 604–609, 2009.

[10] R. Mendoza-Pérez, J. Sastre-Hernández, G. Contreras-Puente, and O. Vigil-Galán, "CdTe solar cell degradation studies with the use of CdS as the window material," *Solar Energy Materials and Solar Cells*, vol. 93, no. 1, pp. 79–84, 2009.

[11] S. S. Liji Sobhana, M. Vimala Devi, T. P. Sastry, and A. B. Mandal, "CdS quantum dots for measurement of the size-dependent optical properties of thiol capping," *Journal of Nanoparticle Research*, vol. 13, no. 4, pp. 1747–1757, 2011.

[12] M. Abdellah, R. Marschan, K. Žídek et al., "Hole trapping: the critical factor for quantum dot sensitized solar cell performance," *Journal of Physical Chemistry C*, vol. 118, no. 44, pp. 25802–25808, 2014.

[13] T. P. Nguyen, T. T. Ha, T. T. Nguyen, N. P. Ho, T. D. Huynh, and Q. V. Lam, "Effect of Cu^{2+} ions doped on the photovoltaic features of CdSe quantum dot sensitized solar cells," *Electrochimica Acta*, vol. 282, pp. 16–23, 2018.

[14] F. Zhuge, X. Li, X. Gao, X. Gan, and F. Zhou, "Synthesis of stable amorphous Cu_2S thin film by successive ion layer adsorption and reaction method," *Materials Letters*, vol. 63, no. 8, pp. 652–654, 2009.

[15] S.-Q. Fan, R.-J. Cao, Y.-X. Xi, M. Gao, M.-D. Wang, and D.-H. Kima, "CdSe quantum dots as co-sensitizers of organic dyes in solar cells for red-shifted light harvesting," *Journal of Optoelectronics and Advanced Materials*, vol. 10, pp. 1027–1033, 2009.

[16] B. Fang, M. Kim, S. Q. Fan et al., "Facile synthesis of open mesoporous carbon nanofibers with tailored nanostructure as a highly efficient counter electrode in CdSe quantum-dot-sensitized solar cells," *Journal of Materials Chemistry*, vol. 21, no. 24, pp. 8742–8748, 2011.

[17] J. Fang, J. Wu, X. Lu, Y. Shen, and Z. Lu, "Sensitization of nanocrystalline TiO_2 electrode with quantum sized CdSe and ZnT_cP_c molecules," *Chemical Physics Letters*, vol. 270, no. 1-2, pp. 145–151, 1997.

[18] G. Chmid, *Nanoparticles: From Theory to Application*, John Wiley & Sons, 2014.

[19] G. Hodes, A. Albu-Yaron, F. Decker, and P. Motisuke, "Three-dimensional quantum-size effect in chemically deposited cadmium selenide films," *Physical Review B*, vol. 36, no. 8, pp. 4215–4221, 1987.

[20] S. Giménez, I. Mora-Seró, L. Macor et al., "Improving the performance of colloidal quantum-dot-sensitized solar cells," *Nanotechnology*, vol. 20, no. 29, p. 295204, 2009.

[21] V. Gonzalez-Pedro, X. Xu, I. Mora-Sero, and J. Bisquert, "Modeling high-efficiency quantum dot sensitized solar cells," *ACS Nano*, vol. 4, no. 10, pp. 5783–5790, 2010.

[22] M. Gratzel, "Photoelectrochemical cells," *Nature*, vol. 414, no. 6861, pp. 338–344, 2001.

[23] M. Gratzel, "Dye-sensitized solar cells," *Journal of Photochemistry and Photobiology C: Photochemistry Reviews*, vol. 4, no. 2, pp. 145–153, 2003.

[24] H. T. Tung, D. Van Thuan, J. H. Kiat, and D. H. Phuc, "Ag+ ion doped on the CdSe quantum dots for quantum-dot-sensitized solar cells' application," *Applied Physics A*, vol. 125, no. 8, 2019.

[25] S. Reghuram, A. Arivarasan, R. Kalpana, and R. Jayavel, "CdSe and CdSe/ZnS quantum dots for the detection of C-reactive protein," *Journal of Experimental Nanoscience*, vol. 10, no. 10, pp. 787–802, 2014.

[26] C. Zhai, H. Zhang, N. du et al., "One-pot synthesis of biocompatible CdSe/CdS quantum dots and their applications as fluorescent biological labels," *Nanoscale Research Letters*, vol. 6, no. 1, 2010.

[27] J. Y. Kim, S. B. Choi, J. H. Noh et al., "Synthesis of CdSe-TiO_2 nanocomposites and their applications to TiO_2 sensitized solar cells," *Langmuir*, vol. 25, no. 9, pp. 5348–5351, 2009.

[28] S. B. Singh, M. V. Limaye, N. P. Lalla, and S. K. Kulkarni, "Copper-ion-induced photoluminescence tuning in CdSe nanoparticles," *Journal of Luminescence*, vol. 128, no. 12, pp. 1909–1912, 2008.

[29] B. B. Srivastava, S. Jana, and N. Pradhan, "Doping Cu in Semiconductor Nanocrystals: Some Old and Some New Physical Insights," *Journal of the American Chemical Society*, vol. 133, no. 4, pp. 1007–1015, 2011.

[30] M. P. A. Muthalif, Y. S. Lee, C. D. Sunesh, H. J. Kim, and Y. Choe, "Enhanced photovoltaic performance of quantum dot-sensitized solar cells with a progressive reduction of recombination using Cu-doped CdS quantum dots," *Applied Surface Science*, vol. 396, pp. 582–589, 2017.

[31] N. S. Karan, D. D. Sarma, R. M. Kadam, and N. Pradhan, *Journal of Physical Chemistry Letters*, vol. 1, no. 19, pp. 2863–2866, 2010.

[32] C. V. V. M. Gopi, M. Venkata-Haritha, S.-K. Kim, and H.-J. Kim, "A strategy to improve the energy conversion efficiency and stability of quantum dot-sensitized solar cells using manganese-doped cadmium sulfide quantum dots," *Dalton Transactions*, vol. 44, no. 2, pp. 630–638, 2015.

[33] K. Veerathangam, M. Senthil Pandian, and P. Ramasamy, "Photovoltaic performance of Pb-doped CdS quantum dots for solar cell application," *Materials Letters*, vol. 220, pp. 74–77, 2018.

[34] K. Veerathangam, M. S. Pandian, and P. Ramasamy, "Photovoltaic performance of Ag-doped CdS quantum dots for solar cell application," *Materials Research Bulletin*, vol. 94, pp. 371–377, 2017.

[35] O. Amiri, M. Salavati-Niasari, and M. Farangi, "Enhancement of Dye-Sensitized solar cells performance by core shell (organic=2-nitroaniline, PVA, 4-choloroaniline and PVP): Effects of shell type on photocurrent," *Electrochimica Acta*, vol. 153, pp. 90–96, 2015.

[36] D. H. Phuc and H. T. Tung, "Quantum dot sensitized solar cell based on the different photoelectrodes for the enhanced performance," *Solar Energy Materials and Solar Cells*, vol. 196, pp. 78–83, 2019.

[37] Y.-J. Shen and Y.-L. Lee, "Assembly of CdS quantum dots onto mesoscopic TiO2films for quantum dot-sensitized solar cell applications," *Nanotechnology*, vol. 19, no. 4, p. 045602, 2008.

[38] W. W. Yu, L. Qu, W. Guo, and X. Peng, "Experimental determination of the extinction coefficient of CdTe, CdSe, and CdS nanocrystals," *Chemistry of Materials*, vol. 15, no. 14, pp. 2854–2860, 2003.